THE ASTROPHYSICAL JOURNAL, 307:760–767, 1986 August 15

A SPECTROPHOTOMETRIC STUDY AND MASS DETERMINATION FOR THE CATACLYSMIC VARIABLE LANNING 10

E. M. SCHLEGEL[1] AND R. K. HONEYCUTT[1]
Indiana University

AND

R. H. KAITCHUCK
Ohio State University

Received 1985 November 22; accepted 1986 February 6

ABSTRACT

We have analyzed time-resolved spectrophotometry of the novalike cataclysmic variable Lanning 10. The radial velocity curves of the He II λ4686 emission line and the *G*-band absorption, coupled with an estimate of the inclination from the continuum eclipse, allow us to derive component masses of $M_{WD} = 0.86 \pm 0.08\ M_{\odot}$ and $M_{RD} = 0.77 \pm 0.04\ M_{\odot}$. The resulting radius of the secondary star places Lanning 10 B on the lower main sequence mass-radius relation. Lanning 10 B does not appear to suffer from the spectral type–mass discrepancy seen in U Gem B and AC Cnc B.

Subject headings: stars: dwarf novae — stars: eclipsing binaries — stars: individual

I. INTRODUCTION

Lanning 10 (=V363 Aur) was discovered by Lanning (1973) in a survey for UV-bright sources using the Palomar Schmidt telescope. Margon and Downes (1981) obtained low-resolution spectra of the system which revealed broad Balmer and He II emission, suggesting that Lanning 10 was a cataclysmic variable. Szkody and Crosa (1981) examined the energy distribution from the ultraviolet to the infrared. They found a flux component due to an F5–G0 main-sequence star $\sim$1 kpc distant, plus a hot (blackbody temperature $>$35,000 K) component which is a characteristic of the accretion disks in cataclysmics.

Horne, Lanning, and Gomer (1982, hereafter HLG) obtained the first detailed spectroscopic and photometric data on Lanning 10. They discovered the system to be eclipsing, with an orbital period of 7^h42^m. In addition, they measured the Hγ radial velocity curve, deriving an amplitude of $\sim$240 km s^{-1}. Flickering was observed to occur with a characteristic period of $\sim$10 minutes. The continuum eclipse curve was analyzed, yielding an inclination of $i \approx 72°$, and an estimate that the accretion disk nearly filled the Roche lobe.

There are a total of five known eclipsing cataclysmic systems which are also double-lined spectroscopic binaries: U Gem, AC Cnc, BD Pav (Barwig and Schoembs 1983), EM Cyg, and Lanning 10. Radial velocity solutions for both components have been obtained for U Gem (Wade 1981), EM Cyg (Robinson 1974), and AC Cnc (Schlegel, Kaitchuck, and Honeycutt 1984); BD Pav's secondary radial velocity curve has not been measured as of this writing. Thus, Lanning 10 is only the fourth eclipsing cataclysmic for which the masses can be found directly with a minimum number of assumptions.

II. OBSERVATIONS

Lanning 10 was observed with the IIDS on the 2.1 m telescope at KPNO on the nights of 1984 December 31 and 1985 January 2, 3, 4, and 5 (UT). A total of 224 spectra were collected with exposure times of 300 s. The entrance aperture was 8″.4, and the seeing disk was much smaller, allowing absolute spectrophotometry. Frequent observations of spectrophotometric standards were made for flux calibration. The bandpass was $\sim$4230–$\sim$4915 Å and the resolution was $\sim$2.5 Å.

The light elements given in HLG were clearly incorrect at this epoch, as the first eclipse was observed to occur $\sim 1^h.3$ earlier than the HLG ephemeris predicted. Table 1 lists the times of minima as given by HLG (entries 1–5), in addition to our times of minima (entries 6–9). Our times of minima were determined by a parabolic fit to integrated flux measurements near minimum. A least-squares solution to all times then gives the ephemeris

$$\mathrm{HJD} = 2{,}444{,}557.9495\ (\pm 6) + 0^d.32124246\ (\pm 20)\mathrm{E}\ .$$

If the cycle count between the two epochs is reduced by 1, a slightly different period is produced ($P = 0^d.32131144\ [\pm 20]$). The values of $O-C$ for this latter period are larger, but only by a factor of 2.

III. DATA REDUCTIONS

The 224 spectra were first examined for orbit-to-orbit variations; since none were seen, the data were co-added into 25 phase bins each 0.04 wide. The first bin is centered on phase 0.0. A gray-scale image of the results is shown in Figure 1. (This gray-scale image has been printed using a Bell and Howell digital gray-scale recorder. The continuum curvature has been removed and the resulting flat continuum set to a common gray level for each co-added spectrum. The continuum eclipse therefore does not appear in the reproduction. The co-added spectra are repeated for one-half cycle to allow continuous display through phase 0.0.) Emission lines of Hγ, He II λ4686, and Hβ are clearly visible. The hydrogen lines shows obvious, albeit chaotic, structure. The He II line is single-peaked and shows the orbital motion of the white dwarf. There is also weaker emission present at the C–N 4645 complex. *G*-band

[1] Visiting Astronomer, Kitt Peak National Observatory, National Optical Astronomy Observatories, which is operated by the Association of Universities for Research in Astronomy, Inc., under contract with the National Science Foundation.

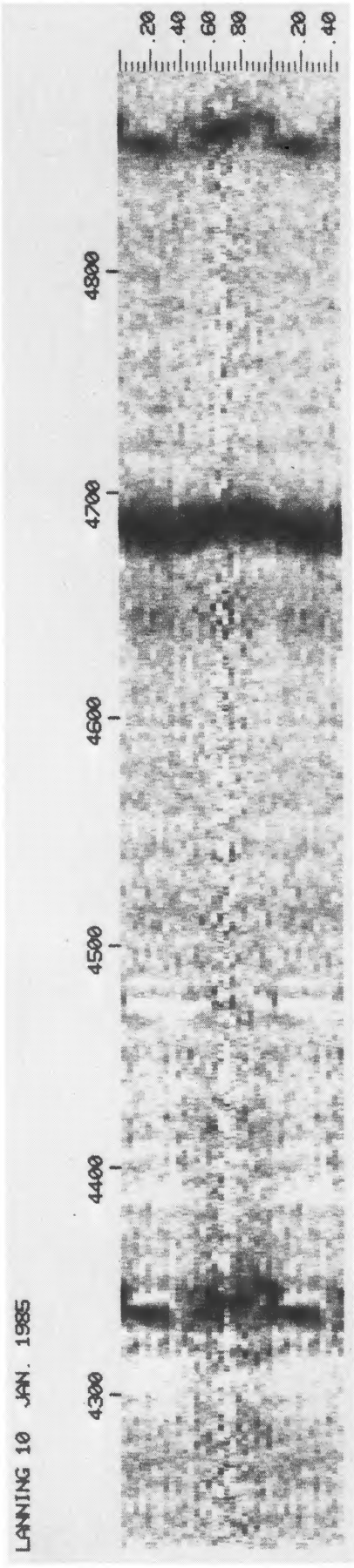

FIG. 1.—Gray-scale reproduction of the time-resolved spectrophotometry of Lanning 10

TABLE 1

TIMES OF MINIMA

Cycle No.	Mideclipse HJD −2,400,000	Old $O-C$ (minutes)	New $O-C$ (minutes)
1. 0.....	44,557.9495	−0.04	+0.64
2. 3.....	44,558.9128	−0.74	−1.26
3. 6.....	44,559.8772	+0.11	−0.29
4. 105.....	44,591.6813	+0.21	+1.29
5. 106.....	44,592.0023	−0.21	+0.95
6. 4694.....	46,065.8614	−73.62	−0.93
7. 4700.....	46,067.7877	−76.48	−2.59
8. 4703.....	46,068.7544	−71.02	+1.69
9. 4706.....	46,069.7182	−71.95	+1.79

NOTE.—Entries 1–5 from HLG.

absorption at 4308 Å is visible, revealing the presence of the secondary component. Also visible are weak absorption lines of He I at 4387, 4471, and 4713 Å, Fe I absorption at ~4405 Å (which appears to be antiphased relative to the He II emission), and a weak absorption line at ~4481 Å, probably Mg II.

A continuum light curve, formed by summing all fluxes in the channels not containing emission lines is shown in Figure 2. The eclipse is ~0.83 mag deep and ~0.1 full width. A weak hump in the light curve just before eclipse, attributed to the disk spot in the canonical model, is also present. We see no evidence of a conventional S-wave in the spectra, and no asymmetry is seen in the eclipse branches.

The He II λ4686 emission line eclipse curve is shown in Figure 3. The He II intensities were established by Gaussian fits to the line and adjacent continuum. There appears to be a weak He II eclipse, centered on the continuum eclipse. The He II eclipse has a depth of ~0.6 mag and a full width of ~0.07 phase units. The He II radial velocity curve, shown in Figure 4, was obtained by fitting a Gaussian profile to the complete line. It is representative of an entire set of radial velocity curves which were generated by excluding various amounts of the core of the line. The fits were made with core exclusions of 0 km s^{-1} (Fig. 4) and exclusion from 350 to 600 km s^{-1} in 50 km s^{-1} increments. (The average HWZI of He II is ~650 km s^{-1}.) Plots of K_{WD} versus excluded velocity, and σ_K (the error in K_{WD}) versus excluded velocity, were constructed, following the example of Shafter (1983). The amplitude initially drops from a value of ~200 km s^{-1} (at 0 km s^{-1} exclusion) to a value of 157 km s^{-1} (at 350 km s^{-1} exclusion). The amplitude and σ_K are then rather constant for all core exclusions except the final exclusion of 600 km s^{-1}. At this core exclusion, σ_K increased drastically. The adopted white dwarf radial velocity amplitude was then taken to be that amplitude corresponding to the last σ_K before the σ_K curve increased, or 162 (±6) km s^{-1}. This value is lower than the value of 240 ± 17 km s^{-1} found by HLG from their 24 spectra. We also find a different γ-velocity (10.1 ± 4.0 km s^{-1} vs. HLG's −61 km s^{-1}) and a smaller phase shift 0.05 ± 0.005 vs. the HLG value of 0.07). HLG attributed the phase lag to enhanced emission associated with the bright spot on the trailing side of the disk. Table 2 lists the adopted radial velocity data, together with other relevant spectroscopic quantities.

The hydrogen lines will not be examined in detail because the Balmer emission is extremely chaotic and shows little orbital motion. It is apparent from Figure 1 that the blue Hγ and Hβ components are much stronger than the red components at most phases, possibly as a result of a wind contribution from the accretion disk (Honeycutt, Schlegel, and Kaitchuck 1986). Also, there is some absorption below the continuum present between the disk components at Hγ and possibly at Hβ. From phase ~0.5 to ~0.9, central emission fills in between the components. This behavior bears a superficial resemblance to S-wave emission which is seen face-on at about phase 0.7. This phasing is approximately correct for the expected impact point of a stream. However, this central Balmer emission does not show the radial velocity behavior expected for an S-wave crossing between the two disk components. Furthermore, because we do not have continuous phase coverage on any one cycle, we cannot rule out a situation in which the central emission is simply contributed by a single random episode of flaring. We note, however, that the visual appearance of the central Balmer emission bears a striking resemblance to the behavior in AC Cnc (Schlegel, Kaitchuck, and Honeycutt 1984). The AC Cnc behavior is in fact synchronized with phase, suggesting a similar situation for Lanning 10.

The major absorption feature visible in Figure 1 is the *G*-band near 4308 Å. (The orbit-averaged *G*-band strength, after removing the red dwarf's motion, may be seen in Fig. 6 [*top*].) Using a cross-correlation technique, we have derived the radial velocity curve of the *G*-band for Lanning 10's secondary. The cross-correlation made use of a spectrum of 70 Oph A (K0 V) obtained using the IIDS. The result is shown in Figure 5. We find $K_{RD} = 181 \pm 5$ km s^{-1}, $\gamma = 35 \pm 3$ km s^{-1}, and a phase shift of -0.070 ± 0.005 from the expected phase of conjunction. An attempt was made to use the He I λ4471 line, but the derived velocity did not define a well-behaved velocity curve.

IV. INCLINATION, MASSES, AND SECONDARY SPECTRAL TYPE

The continuum eclipse width can be used to place limits on the system inclination. Since the eclipse is rather deep, we assume that most of the inner accretion disk is occulted. A

TABLE 2

SPECTRAL LINE INFORMATION

Line	K (km s^{-1})	γ^a (km s^{-1})	$\Delta\phi$	Averaged Line Flux (ergs s^{-1} cm^{-2})	FWHM (Å)
He II λ4686:					
Full profile.....	200 ± 4	18 ± 3	0.040 ± 0.003	0.475×10^{-13}	~15.6
Wings only	162 ± 6	10 ± 4	0.050 ± 0.005	...	...
G band	181 ± 5	35 ± 3	−0.570 ± 0.004	...	~4
Hβ, Hγ.....	~90	~25	~0.04	$\sim 0.20 \times 10^{-13}$	~10

[a] Velocity reduced to the Sun.

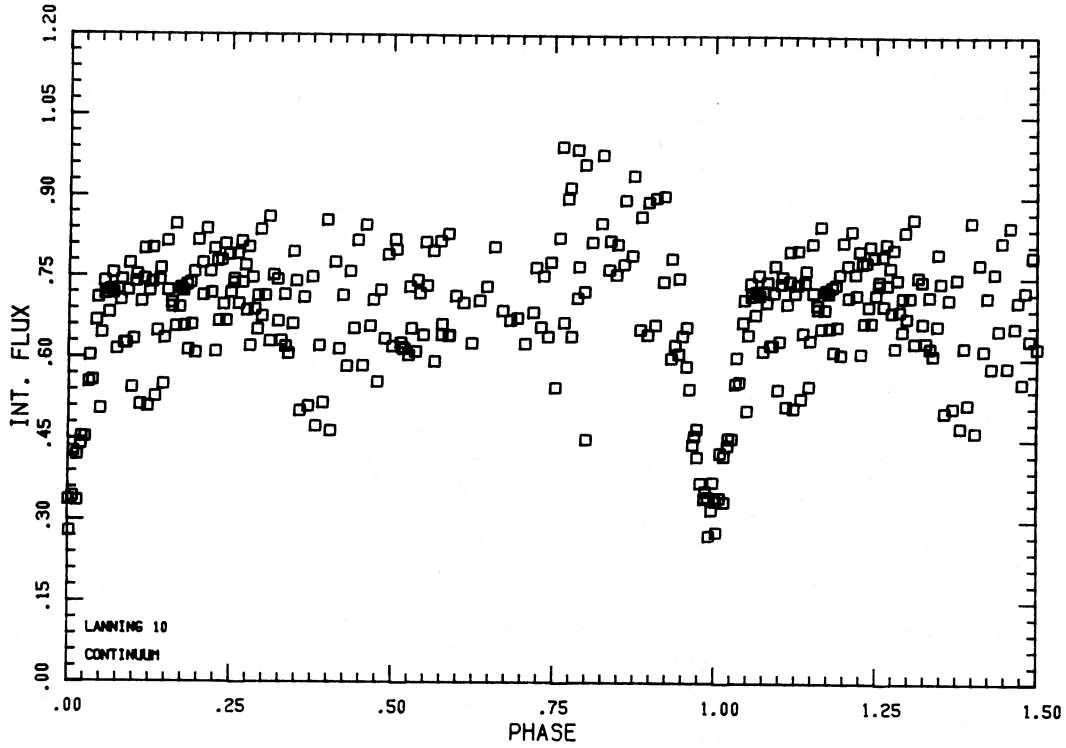

FIG. 2.—Continuum light curve for Lanning 10. The vertical scale is in units of 5.0×10^{-12} ergs s^{-1} cm^{-2}.

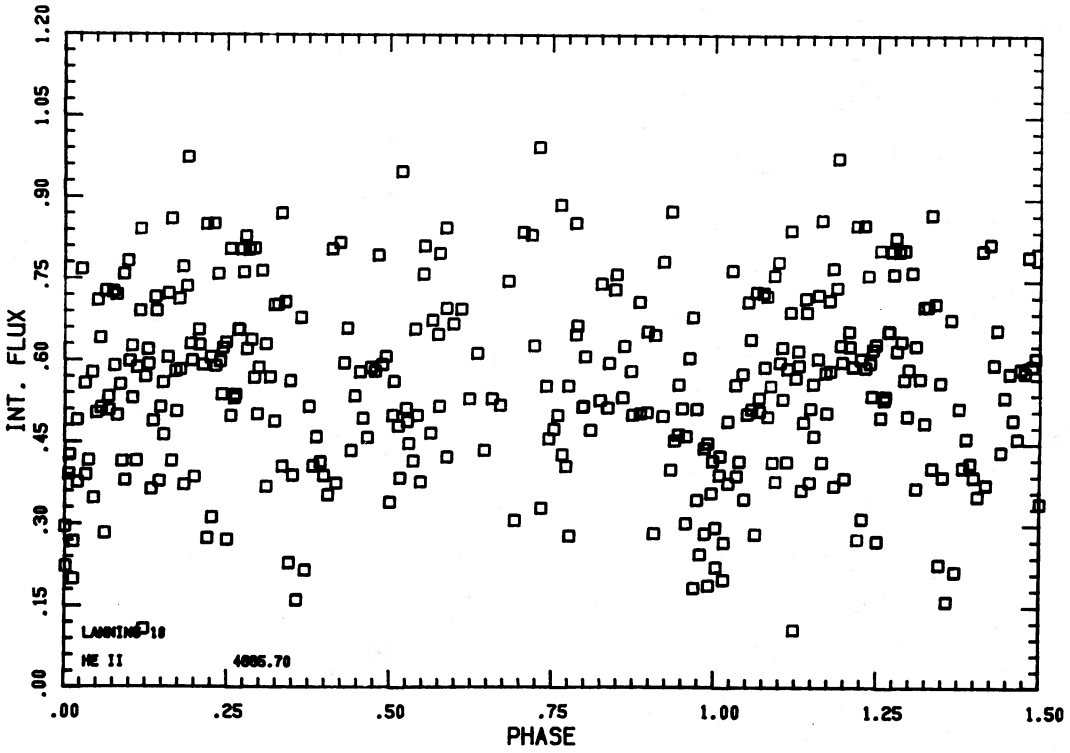

FIG. 3.—He II emission line light curve. The vertical scale is in units of 8.5×10^{-14} ergs s^{-1} cm^{-2}.

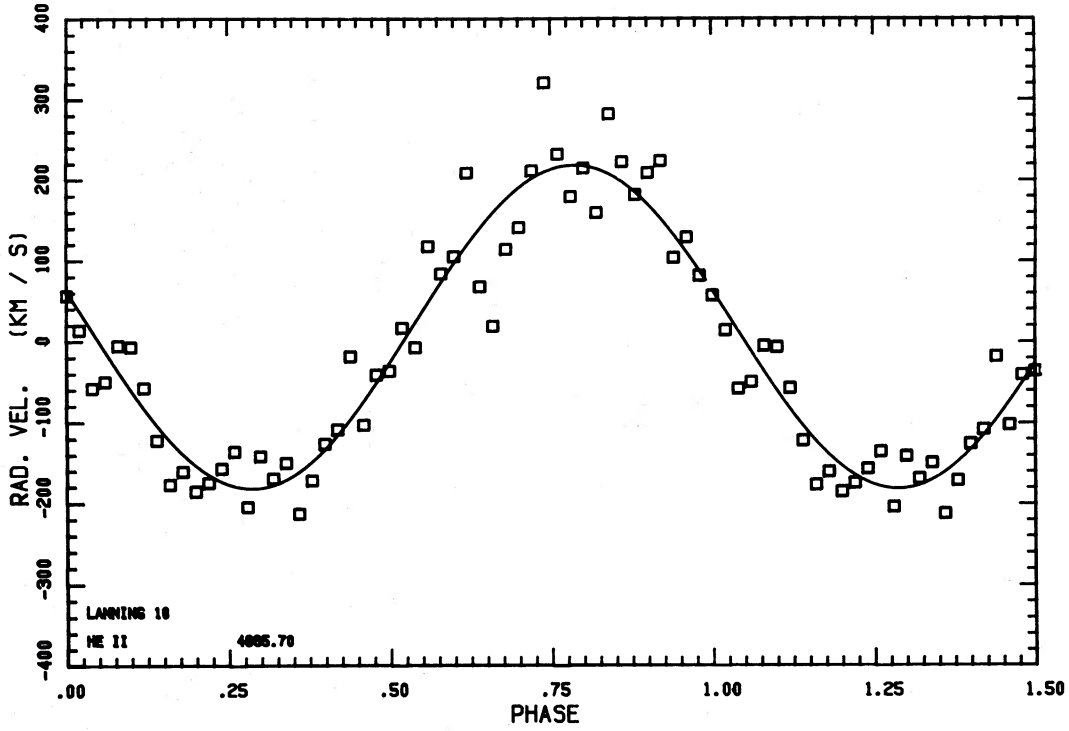

FIG. 4.—Radial velocity curve of He II. This curve was derived without excluding any portion of the line. Radial velocity curves derived with core exclusion look very similar, but are of lower amplitude.

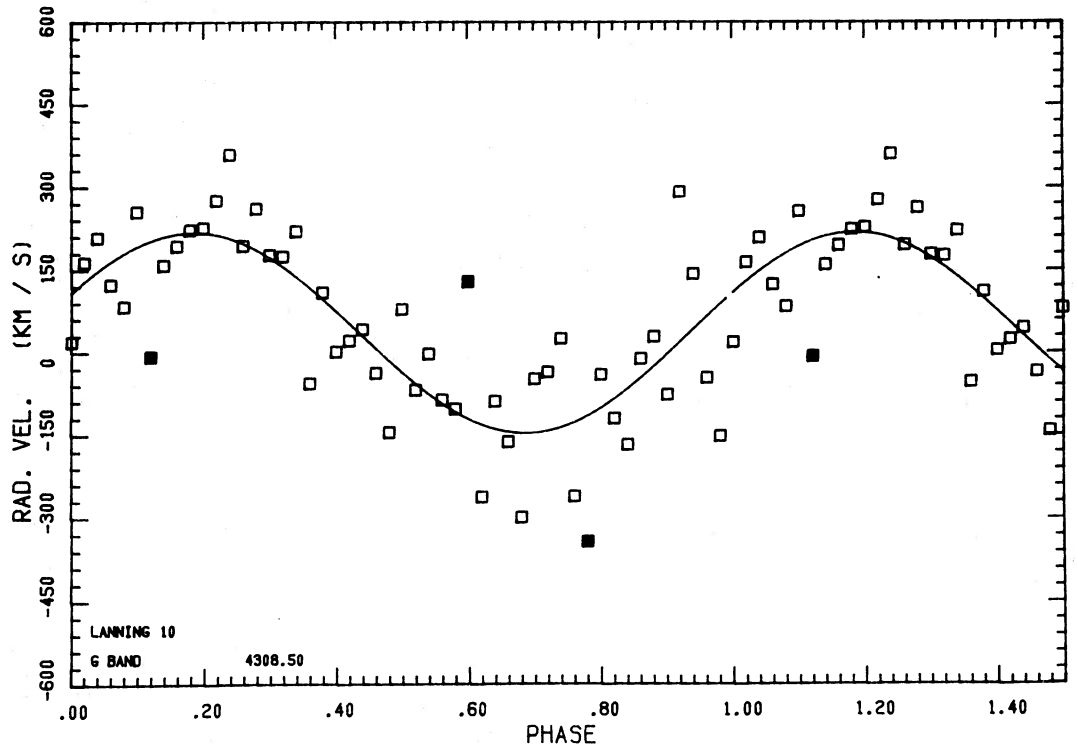

FIG. 5.—Radial velocity curve of the *G* band for the 50 bin co-added data. Line center was determined by a cross-correlation with the K0 V star 70 Oph A. Filled squares were not included in the fit.

TABLE 3

LANNING 10 SYSTEM PARAMETERS

Parameter	Value
P	$0^d32124246$ (± 20)
$q = M_{WD}/M_{RD}$	1.12 ± 0.04
i	$70° \pm 2°$
a	$1.61(\pm 0.05) \times 10^6$ km
M_{WD}	$0.86\ (\pm 0.08)\ M_\odot$
M_{RD}	$0.77\ (\pm 0.04)\ M_\odot$
R_{RD}	$0.83\ (\pm 0.04)\ R_\odot$
R_{disk}	$0.16 \pm 0.04a$
V_{disk}	400 km s^{-1}

lower limit, then, results from an inclination which will allow an occultation of the white dwarf and inner disk, namely,

$$i > \cos^{-1}(R_{RD}/a)\ ,$$

where R_{RD} is the red dwarf radius, and a is the stellar separation. Using the relation of Plavec (1968) for stars filling their Roche lobes,

$$R_{RD}/a = 0.38 - 0.2 \log q\ ,$$

and, using our derived value of $q = M_{WD}/M_{RD} = 1.12 \pm 0.04$, we find $i > 68° \pm 0.5$.

An upper limit for i follows by treating the white dwarf/accretion disk as a spherical star (Kaitchuck, Honeycutt, and Schlegel 1983). For the value of q given above, we find $i < 72° \pm 1$, where the range results from the range in q. We adopt an inclination of $70° \pm 2$ for the mass values which follow, consistent with HLG's value of $i = 72°$.

From our inclination estimate and the observed radial velocity amplitudes, we derive masses of the two stars of $M_{WD} = 0.86 \pm 0.08\ M_\odot$ and $M_{RD} = 0.77 \pm 0.04\ M_\odot$ (error values are formal only). An immediate consideration is whether the secondary fits the lower main sequence mass-radius relation. From our values of a, i, and q, and using $R_{RD}/a = 0.38 - 0.2 \log q$, we find $R_{RD} = 0.86\ R_\odot \pm 0.12$. A comparison with the empirical, lower main sequence mass-radius relation of Patterson (1984) shows Lanning 10 to lie on this relation. The mass and radius of Lanning 10 are also consistent with values for the secondaries of the cataclysmics EM Cyg (Robinson 1974) and AC Cnc (Schlegel, Kaitchuck, and Honeycutt 1984). Finally, we may compare our derived mass estimate with other, indirect, mass-estimating relations. Kiplinger (1979) gives a relation from which the secondary mass may be calculated using the period and mass ratio; for Lanning 10, the secondary mass is predicted to be $0.96\ M_\odot$. Robinson (1976) gives a similar relation which predicts a mass of $1.01\ M_\odot$. Neither relation is particularly accurate for Lanning 10 B.

An estimate of the continuum disk size follows from the eclipse analysis using the method described in Schlegel, Kaitchuck, and Honeycutt (1984). The disk radius will be determined by the region of the disk which is optically thick in the blue. Various relationships exist which link the disk radius, the inclination, and the eclipse width (e.g., Longmore *et al.* 1981)

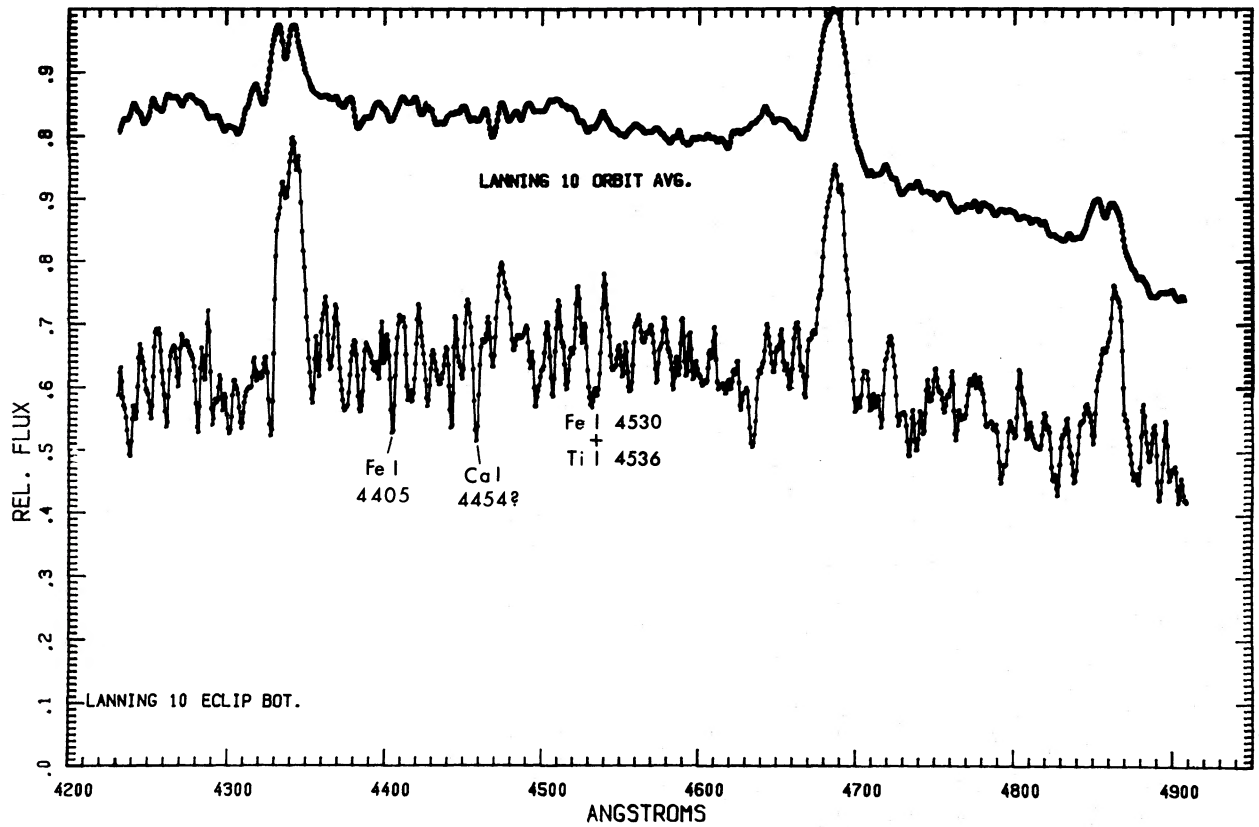

FIG. 6.—(*top*) Orbit-averaged spectrum after removing the red dwarf's motion. The vertical scale is in units of 9.0×10^{-15} ergs s^{-1} cm^{-2} Å^{-1} and is offset by 0.2 relative flux units. (*bottom*) Co-added spectrum of all data at eclipse bottom. Several tentative line identifications are marked. The vertical scale is in units of 0.55×10^{-14} ergs s^{-1} cm^{-2} Å^{-1}.

yielding the results listed in Table 3. The calculated value for the disk radius can be compared to the disk size required by assuming Keplerian motion in the disk (Robinson 1976), namely,

$$r_d = \left(\frac{K_{\rm WD}}{v_d \sin i}\right)^2 (1+q)q \ ,$$

with $q = M_{\rm WD}/M_{\rm RD}$. The value obtained is $r_d \approx 0.44a$, compared to the Roche lobe radius for $q = 1.12$ of $0.41a$ (Plavec and Kratochvil 1964).

Finally, in Figure 6 we have co-added several spectra at the bottom of the eclipse, to look for signs of the secondary. The spectral type cannot be later than ~K3 V, otherwise the wide Mg H λ4790 band would appear. Based on the strengths of Fe I λ4405, Ca I λ4454, and the Fe I λ4530/Ti I λ4536 blend, we can limit the spectral type to late G. The derived mass and radius of the secondary suggest a spectral type near K0 V (Allen 1973). Thus, Lanning 10 B does not appear to suffer from the discrepancy between the surface temperature and the mass, as do U Gem B (Stover 1981; Wade 1979) and AC Cnc B (Schlegel, Kaitchuck, and Honeycutt 1984). In both those secondaries, the calculated mass of the secondary implies a spectral type much earlier than the observed spectrum at the bottom of the eclipse.

This work was supported by NSF grants AST 82-11517 and AST 84-13573.

REFERENCES

Allen, C. 1973, *Astrophysical Quantities* (3d ed.; London: Athlone).
Barwig, H., and Schoembs, R. 1983, *Astr. Ap.*, **124**, 287.
Honeycutt, R. K., Schlegel, E. M., and Kaitchuck, R. H. 1986, *Ap. J.*, **302**, 388.
Horne, K., Lanning, H., and Gomer, R. 1982, *Ap. J.*, **252**, 681 (HLG).
Kaitchuck, R., Honeycutt, R. K., and Schlegel, E. M. 1983, *Ap. J.*, **267**, 239.
Kiplinger, A. 1979, *A.J.*, **84**, 655.
Lanning, H. 1973, *Pub. A.S.P.*, **85**, 70.
Longmore, A., Lee, T., Allen, D., and Adams, D. 1981, *M.N.R.A.S.*, **195**, 825.
Patterson, J., 1984. *Ap. J. Suppl.*, **54**, 443.
Margon, B., and Downes, R. 1981. *A.J.*, **86**, 747.
Plavec, M., 1968, *Adv. Astr. Ap.*, **6**, 202.
Plavec, M., and Kratochvil, P. 1964, *Bull. Astr. Inst. Czechoslovakia*, **15**, 165.
Robinson, E., 1974, *Ap. J.*, **193**, 191.
———. 1976. *Ann. Rev. Astr. Ap.*, **14**, 119.
Schlegel, E. M., Kaitchuck, R. H., and Honeycutt, R. K. 1984, *Ap. J.*, **280**, 235.
Shafter, A. 1983, *Ap. J.*, **267**, 222.
Stover, R. 1981, *Ap. J.*, **248**, 684.
Szkody, P., and Crosa, L. 1981, *Ap. J.*, **251**, 620.
Wade, R., 1979, *A.J.*, **84**, 562.
Wade, R., 1981, *Ap. J.*, **246**, 215.

R. K. Honeycutt and E. M. Schlegel: Astronomy Department, Swain Hall West 319, Indiana University, Bloomington, IN 47405

R. H. Kaitchuck: Department of Astronomy, Ohio State University, 174 West 18th Avenue, Columbus, OH 43210